Volume 1, Issue 1, pp 129 - 141, year 2024

Journal of the Egyptian Society for Basic Sciences-Physics (JESBSP)

https://jesbsp.journals.ekb.eg/

Characterization of Nuclear Properties of Fe- based Alloys for Application in Nuclear Domain

Samah A. Al-Shelkamy[1,*] and Fayez El-Hossary[2]

[1]Department of Physics, Faculty of Science, New Valley University
P.O. Box: 72511, New Valley, Egypt.
[2] Physics Department, Faculty of Science, Sohag University, P.O. Box: 82524, Sohag, Egypt.
(*) Corresponding Author's Email: Samah.alshelkmy@sci.nvu.edu.eg,.

Abstract

The basic aim for the current paper is to investigate the influence of addition of three different chemical elements including Tungsten, Aluminum and Cobalt to the Fe-Composite Alloys prepared by the powder technology compared with a reference stainless steel alloy to be applied for the nuclear domain. The nuclear characterization for the selected Fe-alloys is performed against thermal neutrons add to gamma ray. Where, the incident gamma ray has been optimized theoretically against the energy range beginning from [200 to 3000] keV. The study recommends sample S2 Fe-composite alloy as a good thermal neutrons absorber material and suitable shield against gamma ray prepared by powder technology technique for the nuclear domain application.

Keywords: Fe- Alloys, Additives, Nuclear Domain/Applications.

Declarations The authors have no relevant financial or non-financial interests to disclose.

1. Introduction

The nuclear reactor industry and its various applications within its facilities are related to the materials used in building various power reactor regions [1-2], which are variety of special alloys that are used in constructing several parts for the nuclear reactor structure, including shielding and cladding of the reactor itself [3-7].

Each part of the reactor is exposed to a different set of harsh reactions that depend on the nature of the work of this part within the reactor unit [8-9]. Scientists are interested in developing many different alloys that are characterized by improved mechanical and tribo-chemical properties to face physical and chemical corrosion in the critical reactor environment [10-12]. This is in addition to the intense exposure to high temperatures of ionizing and non-ionizing rays of high density and intensity, which clearly affects the efficiency of the alloys used in constructing the reactor parts, which may reduce the expected final output of the total energy produced by the reactor, which is the main goal of this structure [13].

Alloys manufactured using powder technologies have advanced specifications compared to other alloys prepared by traditional techniques like (ESR) [14-15]. This is due to its superior ability to withstand high temperature conditions, which is a major factor in nuclear reactors that must be taken into consideration. The various types of iron alloys are considered the most common types of alloys in the field of various heavy, medical and nuclear industries [16].Their manufacturing using powder technology is considered an advanced and unique technique compared to other old traditional methods due to its superior surface properties, which have been previously tested through many different microstructure measurements. This is in addition to its high impedance to chemical corrosion reactions [17]. Studying the surface properties of the alloys used in building reactors is very important to avoid cracking or voids resulting from the welding processes or other operating conditions [18-19]. Previously, several studies estimated the effect of adding many different elements to different types of iron alloys, as an example Ti, Nb, Ta, and N to reduce their grain growth and their high oxidation resistance [20].

The research methodology involved the estimation of the nuclear capabilities of recently developed Fe-Composite Alloys against neutrons and gamma radiation. Where, three different chemical elements including Tungsten, Aluminum and Coalt have been added as function for

the Fe- based Alloys compared with a reference stainless steel grade for being fabricated for nuclear reactors applications.

2. Materials and Methods

2.1. Samples preparation

The current study includes six samples of different alloys having variable chemical compositions, five of which are prepared by the powder technology for the Fe- Composite Alloys, meanwhile the sixth sample SS6 is a standard stainless steel sample. The five samples were prepared using the powder technology method, so that the required Fe- Composite Alloy powder sample is prepared in the form of pure powder at a rate of up to 99.9%, then the required proportions of the alloy to be prepared are mixed and ground using a mechanical grinder type SPEX CERTI-PREP800-Series, and the grinding process continues for 22 hours. The rotation speed of the device used is fixed at 350 (rpm). The Fe- Composite Alloy samples S1 to S5 are mixed in the proportions required to be prepared as mentioned in Table 1, then compressed using a hydraulic piston at room temperature under pressure of up to 85 bar. After that, the powder green samples are sintered for a full hour inside a completely vacuum oven under the influence of Argon gas at fixed temperature of 1150 Celsius. As for sample SS6, it is the stainless steel grade sample which is purchased from the steel market and its chemical composition is identified using the X-ray fluorescence device [21- 22], as shown in the following table 1. The stainless steel sample SS6 is cut into an equal size for the previous five Fe- Composite Alloy powder samples, so that the dimensions of all samples are the same, the thickness is one mm, and the diameter is one cm for all investigated Fe-Alloy samples. Then the density is calculated for all investigated samples using the Archimedes method within the reference toluene solution.

Table 1. - Chemical concentration for selected Fe-Composite alloys compared with stainless steel alloy SS6

Wt%	S1 (Fe)	S2 (Fe-5W)	S3 (Fe-5W-4Co-Al)	S4 (Fe-5W-2.5Co-2.5Al)	S5 (Fe-5W-4 Al -Co)	SS6 Stainless steel
Fe	0.99	0.94	0.89	0.89	0.89	0.70
W	----	0.05	0.05	0.05	0.05	---
Co	--	--	0.04	0.025	0.01	----
Al	---	--	0.01	0.025	0.04	----
Si	0.01	0.01	0.01	0.01	0.01	0.0435
Cr	----	---	---	---	-----	0.17
Ni	-----	----	----	---	-----	0.086
C	----	-----	----	----	---	0.0005
Density g/cm^3) (	7.691	7.924	7.81	7.58	7.364	7.095

2.2.Nuclear characterization for the investigated alloys

The nuclear characterization for the selected Fe-Alloys is performed theoretically against thermal neutrons add to gamma ray [23-24]. The incident gamma ray has been examined theoretically against the incident energy range beginning from [200 to 3000] keV utilizing the Win X Com program. Where, the selected gamma ray energy lines represent the characteristic gamma radiation belonging to the natural radioactive sources ^{60}Cobalt, ^{137}Cesium and ^{208} Bismuth. To examine the capability for these Fe-Composite alloys to be applied for nuclear applications when compared with the stainless steel grade SS, several radiation shielding parameters are obtained for the investigated alloys against incident nuclear radiation based on Lambert law. These parameters include: gamma radiation mass & linear attenuation coefficients (MAC & LAC) mean free path (MFP) , tenth-value layer thickness (TVL), add to neutrons removal cross section Thermal $\sum$R (cm^{-1}) that has been determined at the energy range (2–12) MeV.

3- Results

Figure 1 shows a histogram of the measured experimental density values for the selected prepared five Fe-Composite alloys by the powder technology making method compared with the other purchased reference stainless steel sample SS6.

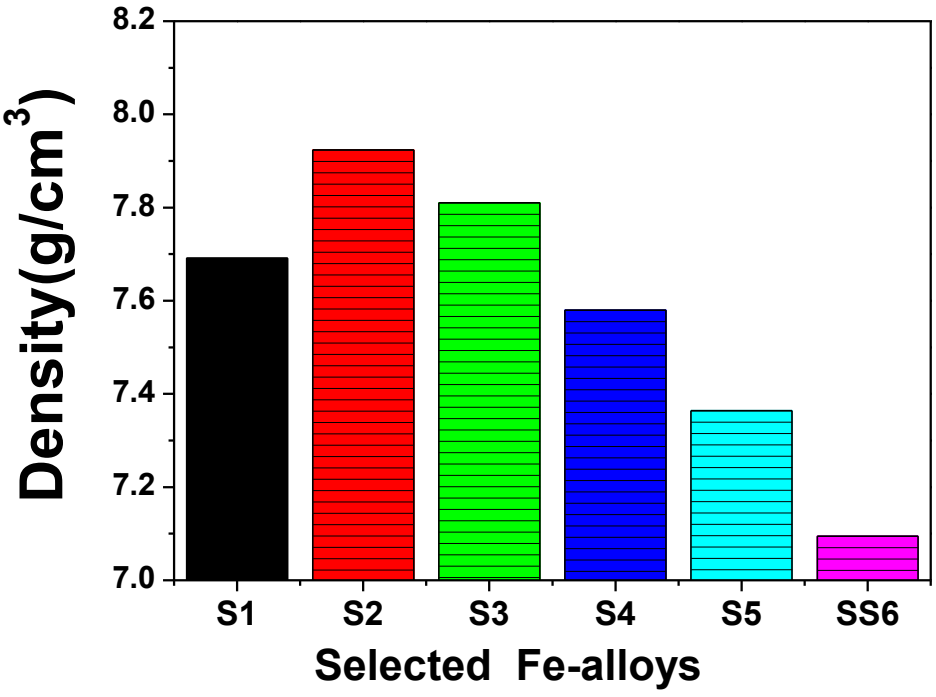

Figure1. Density (cm^2/g) for selected Fe-Composite alloys compared with stainless steel SS6.

The nuclear capabilities for the recently investigated Fe-alloys against incident thermal neutrons and gamma radiation are revealed by the next table 2 and are represented by the following figures from 2 to 6.

Table 2 .(A-E) Nuclear characteristic data for selected Fe-Composite alloys compared with stainless steel SS6 against incident gamma and thermal neutron radiation

A- LAC (cm)						
Gamma energy KeV)(	S1	S2	S3	S4	S5	SS6
283.53	0.019013	0.02242	0.021768	0.021165	0.020873	0.017631
346.93	0.015264	0.016281	0.015778	0.015314	0.015106	0.014094
661.657	0.01379	0.014185	0.013747	0.013329	0.01315	0.012708
826.06	0.010248	0.010016	0.009702	0.00941	0.009278	0.009431
1173.24	0.009236	0.008968	0.008686	0.008425	0.008306	0.008497
1332.5	0.00777	0.007502	0.007265	0.007046	0.006947	0.007147
2614.53	0.007291	0.007034	0.006811	0.006607	0.006513	0.006708

B-HVL (cm)						
Gamma energy KeV)(	S1	S2	S3	S4	S5	SS6
283.53	36.45574	30.91596	31.84276	32.74942	33.20737	39.31412
346.93	45.40978	42.57407	43.93023	45.26321	45.88553	49.17892
661.657	50.26451	48.86621	50.4228	52.00268	52.71112	54.54262
826.06	67.6369	69.20167	71.44487	73.6628	74.70754	73.50055
1173.24	75.04775	77.28991	79.80036	82.27172	83.44725	81.57606
1332.5	89.20514	92.39447	95.40686	98.37324	99.7729	96.98008
2614.53	95.06822	98.54576	101.7636	104.9124	106.4231	103.3339

C-MFP (cm^{-1})						
Gamma energy KeV)(	S1	S2	S3	S4	S5	SS6
283.53	52.59451	44.60231	45.93939	47.24743	47.9081	56.71829
346.93	65.51247	61.4214	63.37793	65.301	66.19883	70.95019
661.657	72.51635	70.49904	72.74472	75.02402	76.04607	78.68836
826.06	97.57943	99.83691	103.0732	106.273	107.7802	106.0389
1173.24	108.271	111.5058	115.1276	118.693	120.3889	117.6894
1332.5	128.6958	133.297	137.643	141.9226	143.9419	139.9127
2614.53	137.1545	142.1715	146.8139	151.3566	153.5361	149.0793

D-TVL (cm)						
Gamma energy KeV)(	S1	S2	S3	S4	S5	SS6
283.53	121.1033	102.7006	105.7794	108.7912	110.3125	130.5987
346.93	150.848	141.428	145.9331	150.3611	152.4284	163.3688
661.657	166.9751	162.33	167.5009	172.7492	175.1025	181.1866
826.06	224.6849	229.883	237.3347	244.7025	248.1731	244.1636
1173.24	249.3032	256.7515	265.0911	273.3008	277.2058	270.9898
1332.5	296.3331	306.9278	316.9347	326.7888	331.4384	322.1609
2614.53	315.8098	327.3619	338.0514	348.5114	353.53	343.2677

R (cm $^{-1}$)∑Thermal E-	
S1	0.16180
S2	0.16189
S3	0.1580
S4	0.15686
S5	0.15349
SS6	0.14892

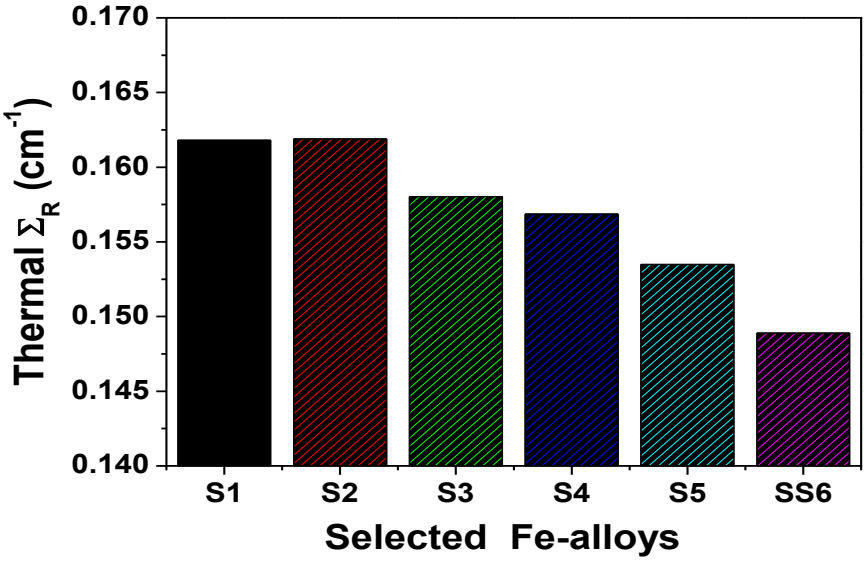

Figure 2. Thermal ∑R (cm^{-1}) neutrons removal cross section for selected Fe-Composite alloys compared with stainless steel SS6.

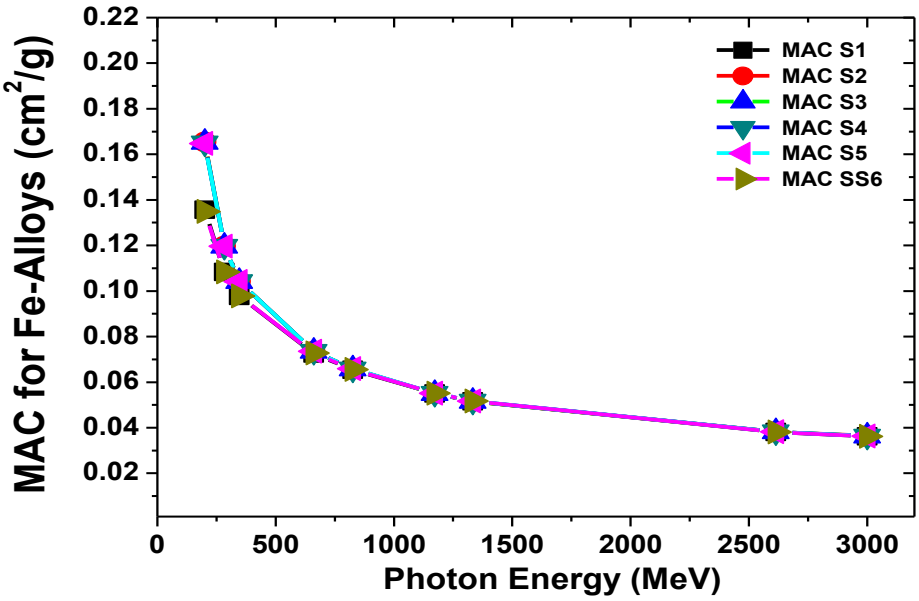

Figure 3. Mass attenuation coefficient (cm^2/g) for selected Fe-Composite alloys compared with stainless steel SS6.

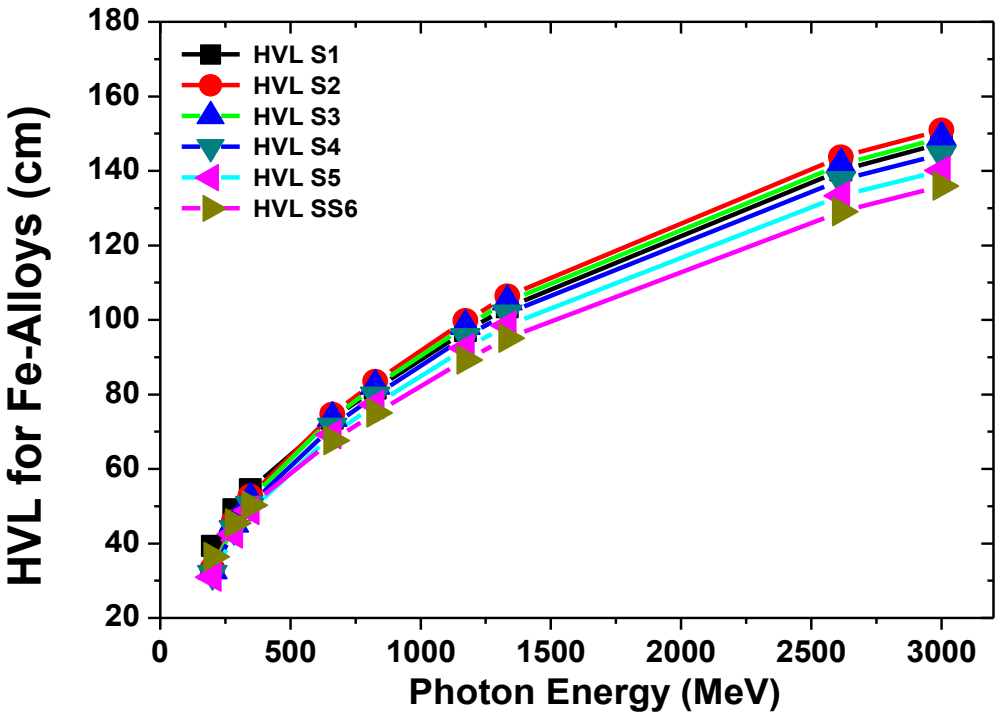

Figure 4. HVL (cm) for selected Fe-Composite alloys compared with stainless steel SS6

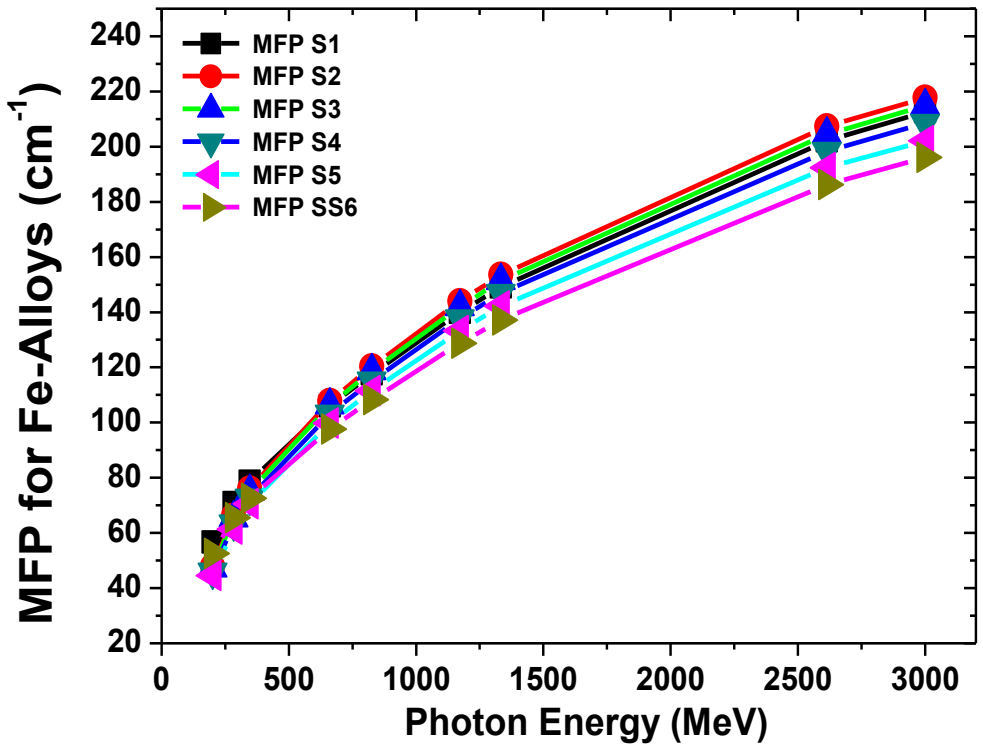

Figure 5. MFP (cm) for selected Fe-Composite alloys compared with stainless steel SS6

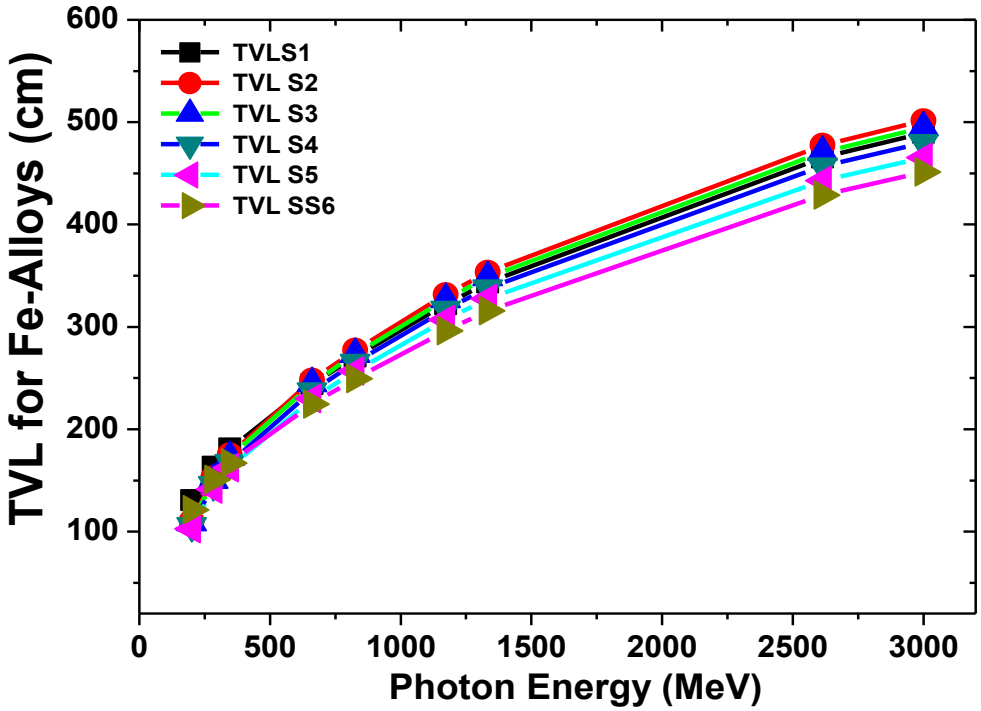

Figure 6. TVL (cm) for selected Fe-Composite alloys when compared with stainless steel SS6

4- Discussion

Figure 1 shows a histogram representing the experimental density values for all the selected Fe–alloys. Where, five of those samples are Fe-Composite alloys prepared by the powder technology method and the Sixth sample SS6 is a reference stainless steel alloy. The first Fe-Composite alloy S1 contains 1% wt of Silicon added to 99% wt iron and has density 7.91 (cm^3/g). The second Fe-Composite alloy S2 contains 1% wt Silicon plus 5 % wt of Tungsten, that are added at the expense of Iron and it has density 7.924 (cm^3/g). As for the third Fe-Composite alloy S3, it also contains 5% wt Tungsten added to 4% wt Cobalt mixed by 1% wt of Aluminum and 1% Silicon, that are added at the expense of Iron .S3 has density 7.81 (cm^3/g). Moving to the fourth Fe-Composite alloy S4, we find that the additive percentages of Aluminum and Cobalt were modified compared to the previous sample S3. Whereas, it contains 2.5 wt% Cobalt as well as 2.5 wt% Aluminum and the concentration of Tungsten continued to be 5 wt% plus 1 wt% silicon, and S4 density was 7.58 (cm^3/g). When we go to the fifth Fe-Composite alloy S5, which is the last alloy of the powder technology prepared samples. The chemical proportions were adjusted. So that, the concentration of Aluminum became 4 wt%, while Cobalt was 1 wt%, and Tungsten was 5 wt%, at the expense of Iron, and its density was 7.364 (cm^3/g). It is clear from figure 1 that, the density ratios for all the Fe-Composite alloy powder samples vary with the difference in the ratios of the chemical composition elements that are making up the alloys. Sample S2 achieved the highest density

and the lowest density belongs to sample S5 among the entire five Fe-Composite alloys. Moving on to the stainless steel sample SS6, which contains more other chemicals added at the expense of Iron, namely Nickel, Chromium, and Cobalt, in addition to slight touches of Carbon, which is a characteristic of reinforced stainless steel alloys . SS6 density is 7.095 (cm^3/g) and it records the lowest density at the entire Fe-alloy group of six samples.

The process of evaluating nuclear properties for the Fe-Composite alloys to be applied for the nuclear domain, begins by investigating Thermal ∑R-neutrons removal cross section (cm^{-1}) for the selected Fe-Composite alloys compared with the reference stainless steel SS6 as revealed in Figure 2. Also, whole Thermal ∑R (cm^{-1}) neutrons removal cross section values are mentioned in detail at Table (2-E). The highest Thermal ∑R (cm^{-1}) neutrons removal cross section value in the five Fe-Composite alloys goes to sample S2 = 0.161898 cm^{-1}, and the lowest value goes to sample S5 = 0.15349 cm^{-1}. Mean while, the reference stainless steel sample S6 records the lowest Thermal ∑R = 0.1489 cm^{-1} at the whole studied six alloys. Where, stainless steel SS6 contains the light element Carbon, and is characterized by its distinguished ability to absorb neutrons and continues to be on the throne of alloys used for repelling thermal neutrons.

Moving on to Gamma ray, that represents the most important radiation type in the field of the nuclear domain. The nuclear distinctive properties for the selected six Fe-alloys under study were evaluated by obtaining the following nuclear shielding coefficients (MAC, LAC, TVL, HVL and MFP) revealed by figures 2 to 6 and their corresponding values are mentioned in detail by table 2.

Those shielding parameters are optimized at the gamma ray energy range (200 to 3000) keV, that represents the spectral lines of gamma rays emitted from the following natural radioactive sources, ^{137}Cesium (283.53 and 661.657), ^{60}Cobalt (346.93, 826.06, 1173.237, 1332.501) and ^{208}Bithmuth (2614.533).

Through Figure 3 and Table 2, it's obvious that the behavior of each of the LAC and MAC radiation shielding parameters decreases as function of the increased incident gamma ray starting from (200 to 3000) keV. Meanwhile, figures 4, 5 and 6 show that HVL, TVL and MFP shielding parameters increase as function of the incident gamma rays at the same mentioned energy range.

As shown from table 2 and figures (3-6) Fe-Composite alloy sample S2 has the highest shielding against the lower gamma ray energy line 238.53 keV emitted from ^{137}Cesium. Where,

the recorded HVL=30.91596 cm and TVL=102.7006 cm. Mean while the weakest shielding for the investigated Six Fe-alloy samples goes to the stainless steel sample SS6. Where, the recorded HVL= 39.314 cm and TVL=130.598 cm.

Fe-Composite alloy sample S1 achieved the highest shielding against the higher gamma ray energy line 2614.53 keV emitted from ^{208} Bismuth. . Where, the recorded HVL=95.068 cm and TVL=315.80 cm. Mean while, the weakest shielding at the same energy range belongs to Fe-Composite alloy sample S5 where the recorded HVL = 105.423 cm and TVL=315.89 cm.

5. Conclusions

The current research paper includes evaluating the impact of adding different concentrations of Tungsten, Aluminum and Cobalt elements to the Fe-based alloys utilizing the powder technology method compared with reference stainless steel alloy SS6 for the nuclear domain applications. Practical density measurements for all investigated alloys reveal that the final density value relies on the chemical composition for the elements making up the final Fe-alloy. The nuclear shielding properties of the samples against thermal neutron rays were evaluated. Sample S2 Fe-composite alloy achieved the highest absorption for thermal neutrons= 0.161898 cm^{-1} and the stainless steel sample S6 records the lowest thermal neutron cross section Thermal $\sum R$ = 0.01489 cm^{-1} and continues to be on the throne of neutron-resistant materials when compared with the other five Fe-composite alloys prepared by powder technology. Going to gamma rays, it was found that the best shielding sample at the lower energy range is S2 and the best for the higher energy range is S1.

6. References

[1] Deng Z, Yang P, Huo Z, Zou L &Wang Y, Comparison and mechanism research of corrosion behaviour of materials used in supercritical water-cooled reactors, The Journal of Supercritical Fluids, **207,** p106192, 2024.
https://doi.org/10.1016/j.supflu.2024.106192.

[2] Ma Y, Chu H & Zheng B, Research progress of plasma melting technology in radioactive waste treatment of nuclear power plants, Annals of Nuclear Energy, **198**, p110307, 2024.
https://doi.org/10.1016/j.anucene.2023.110307.

[3] Eslinger P W, Doll C G, Bowyer T W, Friese J I, Metz L A & Sarathi R S, Impacts of future nuclear power generation on the international monitoring system, Journal of Environmental Radioactivity, **273**, p107383, 2024.
https://doi.org/10.1016/j.jenvrad.2024.107383.

[4] El-Hossary F M, El-Kameesy S U, Eissa M M, Abd El-Moula A A & Al-Shelkamy S A, Influence of Rf plasma carbonitriding on AISI304L, SSMn6Ni and SSMn10Ni for nuclear applications, Materials Research Express, **6(9)**,p 096596,2019.
https://doi.org/10.1088/2053-1591/ab30e2.

[5] El-Kameesy S U, El-Hossary F M, Eissa M M, Abd El-Moula A A, Al-Shelkamy S A & Saeed A (2019, June), Radiation shielding, mechanical and tribological properties of treated AISI304L using H2/N2 rf plasma. In Journal of Physics: Conference Series, IOP Publishing**, 1253** p 012034, 2019.
https:// doi.org/10.1088/1742-6596/1253/1/012034.

[6] Saeed A, Eissa M, El-Hossary F M, EL-Kameesy S U & Elmoula A, Mechanical and gamma ray attenuation properties of N316L steel treated by rf plasma as a nuclear material, Arab Journal of Nuclear Sciences and Applications, **52(2**), p7-12, 2019.
https://doi.org/10.21608/ajnsa.2019.2936.1059.

[7] Al-Shelkamy Samah A, Hashish H M Abu & Salama E, Radiation attenuation, structural, mechanical and lubricant wear analysis against 5% wtNaCl of heat treated stainless steel grades, ISSSD 2021: 21 international symposium on solid state dosimetry, Mexico: Sociedad Mexicana de Irradiacion y Dosimetria, 2021.

[8] El-Kameesy S U, El-Hossary F M, Eissa M M, Abd El-Moula A A & Al-Shelkamy S A, Enhancing the capability of plasma treated austenite stainless steels as thermal reactor materials, Materials Research Express, **6(12)**, p126589, 2019.
https://doi.org/10.1088/2053-1591/ab5a9e.

[9] El-Hossary F M, El-kameesy S U, Eissa, M M, Abd Elmula A A, Saeed A & Al-Shelkamy S A, (2017, December), Effect of Plasma Surface Treatment on AISI 316LStainless Steel for In-Core Applications of Nuclear Reactors, In Proceedings of the 4th International Conference on Energy Engineering, Aswan, Egypt , p26-28, 2017.

[10] Monazie A M, Al Kaisy A M, Tawfic A F & Al-Shelkamy S A, Shielding and dosimetry parameters for aluminum carbon steel, Applied Radiation and Isotopes, **201**, p111022, 2023.
https://doi.org/10.1016/j.apradiso.2023.111022.

[11] Moosa M H, Abu-Okail M, Abu-Oqail A, Al-Shelkamy S A, Shewakh W M & Ghafaar M A, Structural and Tribological Characterization of Carbon and Glass Fabrics Reinforced Epoxy for Bushing Applications Safety, Polymers, **15**(9), 2064, 2023.
https://doi.org/10.3390/polym15092064.

[12]Al-Shelkamy S A, Abu Hashish H M & Mahdy A A, Structural and Tribological Properties of Heat-Treated Stainless Steels against Abrasive and Lubricant Wear Conditions, Coatings, **11(12),** p1473, 2021.
https://doi.org/10.3390/coatings11121473.

[13] Kessler G, Veser A, Schlüter F H, Raskob W, Landman C & Päsler-Sauer J, The risks of nuclear energy technology, Safety Concepts of Light Water Reactors, Springer: Berlin/Heidelberg, Germany, 2014.

[14] Dutt B S, Babu M N, Ganesan V, Shanthi G& Moitra A, Prediction of Fracture Resistance from Tensile Properties and Validation with Experimental Data for 316 Type Stainless Steels, Journal of Materials Engineering and Performance, p 1-14, 2024.
https://doi.org/10.1007/s11665-024-09140-z.

[15] Al-Shelkamy Samah A, Abu Hashish H M & Salama E, Influence of heat treatment on the mechanical and the lubricant wear characteristics of stainless-steel grades against 5 wt% NaCl as industrial shielding materials, Appl. Radiat. Isot, **188,** p1–4, 2022. https://doi.org/10.1016/j.apradiso.2022.110361.

[16] Ge Y, Chang L, Bojinov M, Saario T & Que Z, Mechanistic understanding of the localized corrosion behavior of laser powder bed fused 316L stainless steel in pressurized water reactor primary water, Scripta Materialia, **238**, p115764, 2024.
https://doi.org/10.1016/j.scriptamat.2023.115764.

[17] Pan Y, Yang Y, Zhou Q, Qu X, Cao P & Lu X, Achieving synergy of strength and ductility in powder metallurgy commercially pure titanium by a unique oxygen scavenger, Acta Materialia, **263**, p 119485, 2024.
https://doi.org/10.1016/j.actamat.2023.119485.

[18] Li H, Zhang D, Qin H, Li X, Deng J, Tian W, ... & Qiu S, Study on tritium transport characteristics in fluoride-salt-cooled high-temperature advanced reactor, International Journal of Hydrogen Energy, **56**, p1101-1110, 2024.
https://doi.org/10.1016/j.ijhydene.2023.12.199.

[19] Al-Shelkamy Samah A & El-Hossary F M, Radiofrequency Plasma surface engineering method Stainless steel alloy for the Nuclear Power Plant Unit, ISSSD 2022, international symposium on solid state dosimetry, Mexico: Sociedad Mexicana de Irradiacion y Dosimetria, 2022.

[20] Sun X, Fan Y, Nie J, Chen Y, Xie K, Liu S, ... & Liu X, Significant improvement of the room and cryogenic mechanical properties of an AlN particle reinforced Al matrix composite by alloying element magnesium, Composites Part B: Engineering, **268**, p111056, 2024. https://doi.org/10.1016/j.compositesb.2023.111056.

[21] Al-Shelkamy S A, Mosa E S, Mahdy A A & Elkady O, Studies on heavy tungsten materials manufactured by Powder technology for Nuclear applications, ISSSD 2022, international symposium on solid state dosimetry, Mexico: Sociedad Mexicana de Irradiacion y Dosimetria, 2022.

[22] Al-Shelkamy Samah A & Vega-Carrillo H R, Evaluating Shielding Properties of Medium Entropy Alloys for Modern Nuclear Energy Applications, ISSSD 2023, international symposium on solid state dosimetry, Mexico: Sociedad Mexicana de Irradiacion y Dosimetria, 2023.

[23] Al-Shelkamy S A, Vega-Carrillo H R, Xie Z, El-Hossary F M, Mosa E S, Mahdy A A, ... & Ghafaar M A, Mechanical and radiation shielding characterization of W-based alloys for advanced nuclear unit, Applied Radiation and Isotopes**, 201,** p110995, 2023. https://doi.org/10.1016/j.apradiso.2023.110995.

[24] Al-Shelkamy Samah A, El-Hossary F M, Vega-Carrillo H R, Mosa E S, Daha M A, Ghafaar M A, & Abd El-Moula A A, Improving the properties of commercial steel alloys in the industrial/nuclear field by RF plasma carbonitriding, Applied Radiation and Isotopes, **193**, 110619, 2022. https://doi.org/10.1016/j.apradiso.2022.110619.